

# Design of a Control System for Hybrid Quadcopter Tilt Rotor Based on Backward Transition Algorithm

Purwadi Agus Darwito <sup>1\*</sup>, Nilla Perdana Agustina <sup>2\*</sup>, Hudzaifa Dhiaul Ahnaf <sup>3</sup>, Syahrizal Faried Roosydi <sup>4</sup>,  
 Detak Yan Pratama <sup>5</sup>, Totok Ruki Biyanto <sup>6</sup>

<sup>1, 2, 3, 4, 5, 6</sup> Department of Engineering Physics, Sepuluh Nopember Institute of Technology, Surabaya, Indonesia

Email: <sup>1</sup> padarwito@ep.its.ac.id, <sup>2</sup> 7009231002@mhs.its.ac.id, <sup>3</sup> ahnafhudzaifa@gmail.com, <sup>4</sup> fariedsyahrizal@gmail.com,  
<sup>5</sup> detak@ep.its.ac.id, <sup>6</sup> trb@ep.its.ac.id

\*Corresponding Author

**Abstract**—An Unmanned Aerial Vehicle (UAV) is an unmanned aerial vehicle that can be controlled using either automatic or manual control. UAVs are divided into two types: rotary-wing, which uses rotating propellers to fly the aircraft, and fixed-wing, which uses fixed wings to fly the aircraft. One of the advanced developments in UAV technology is the Hybrid Vertical Take-Off Landing Quadrotor Tiltrotor Aircraft (QTRA) system, which combines the quadrotor UAV system, classified under rotary-wing, with the fixed-wing UAV system. This allows for vertical takeoff and landing as well as the ability to cruise at maximum speed. In the transition between flight modes, from quadcopter to fixed-wing and vice versa, the transition is carried out by changing the thrust direction of the two front UAV rotors from horizontal to vertical and vice versa. The change in thrust angle on the rotor is referred to as a tilt rotor. The problem that arises from changing the aircraft mode from fixed-wing to quadcopter is controlling the UAV's transition mode, which must not lose its lift force. Therefore, the tilt angle must be changed as quickly as possible. To solve this issue, a Hybrid VTOL Quadrotor Tiltrotor aircraft concept was designed with fast response, controlled by a Proportional Derivative (PD) controller. The results of the PD control system were tested in simulations by observing the X and Z positions of the UAV, which can stabilize the position during the transition. The success criteria targeted for a stable response include a tilting angle with a settling time of 7 seconds, an overshoot height of 16 meters, and a steady-state error approaching zero. From the transition simulation tests, the system response data showed performance with an X-axis settling time of 37 seconds, a steady-state error value of 0.1 meters, and an overshoot of 0.4%.

**Keywords**—Hybrid VTOL Tilt-rotor; MAV; Proportional Derivative Control; UAV Backward Transition.

## I. INTRODUCTION

Unmanned Aerial Vehicles (UAVs) have advanced rapidly over the past few decades [1]–[3]. UAVs have been widely used in various sectors, including the military [4]–[6], industry [7]–[9], and other commercial sectors [10]–[12]. UAV technology continues to evolve, both in terms of hardware and software, to enhance its efficiency, safety, and operational capabilities [13]–[16]. Some types of UAVs based on design include fixed-wing [17][18], rotary-wing [19][20], and hybrid [21]–[24]. An overview of the strengths and weaknesses of each type of UAV, focusing on efficiency, flexibility, and challenges in operation and control, is presented in Table I.

TABLE I. COMPARISON OF EACH TYPE OF UAV

Type of UAV	Advantages	Disadvantages
Fixed Wing	<ul style="list-style-type: none"> <li>- High energy efficiency, ideal for long-distance flights.</li> <li>- Capable of flying for longer durations with larger payloads.</li> <li>- More stable at high speeds and in adverse weather conditions.</li> </ul>	<ul style="list-style-type: none"> <li>- Cannot perform hovering (stay in one place).</li> <li>- Requires a runway for takeoff and landing.</li> <li>- Limited maneuverability compared to other types (less flexible).</li> </ul>
Rotary-Wing	<ul style="list-style-type: none"> <li>- Capable of hovering, vertical take-off, and landing (VTOL).</li> <li>- Highly flexible for maneuvers in tight or limited spaces.</li> <li>- Does not require a runway.</li> </ul>	<ul style="list-style-type: none"> <li>- Higher energy consumption, resulting in shorter flight duration.</li> <li>- Less efficient for long-distance flights compared to fixed-wing.</li> <li>- More susceptible to strong winds or adverse weather conditions.</li> </ul>
Hybrid (Tilt-Rotor)	<ul style="list-style-type: none"> <li>- Combines the advantages of fixed-wing and rotary-wing, capable of VTOL and long-distance flight.</li> <li>- Better efficiency than rotary-wing, especially for long-distance flights.</li> <li>- Flexible for various applications (hovering and long-distance flight).</li> </ul>	<ul style="list-style-type: none"> <li>- More complex and expensive system.</li> <li>- Maintenance and control are more complicated due to the mode transition.</li> <li>- Vulnerable to errors during the transition phase (changes in flight mode).</li> </ul>

The hybrid quadcopter tilt rotor is one of the latest innovations in UAV technology, combining the hovering capability and flexible maneuverability of quadcopters with the long-distance flight efficiency of fixed-wing aircraft [25]–[27]. This design allows the rotors to change position or tilt, enabling a seamless transition between fixed-wing and multirotor flight modes [28]–[31]. This capability makes the hybrid tilt rotor quadcopter highly attractive for applications that require long-distance flight efficiency as well as vertical takeoff and landing capabilities. In UAV systems, the transition phase also plays a crucial role, especially in the operation of hybrid tilt rotor quadcopters [32]–[35]. This type of UAV has the ability to switch between hover mode (vertical flight) and cruise mode (horizontal flight), which requires a change in rotor configuration during the transition. One of the most critical transition phases is when the tilt rotor quadcopter switches to the landing phase [36]–[38]. The aerodynamic dynamics change significantly, especially when



the UAV transitions backward toward landing [39]–[41]. The backward transition in a hybrid tilt rotor is the process in which the rotors of the tilt rotor aircraft rotate backward as the aircraft switches from vertical flight mode (VTOL) to horizontal flight mode (forward flight) [42]–[44]. Similar to the delivery process, UAVs must be able to maneuver accurately when approaching the delivery point. This involves transitioning from cruise mode, where the UAV is moving quickly through the air, to hover mode to lower the cargo [45]–[47]. Instability during this transition phase can lead to delivery failures or even accidents if the UAV is not controlled properly [48]–[50]. For monitoring or surveying, UAVs often need to switch from hover mode for detailed observation to cruise mode to quickly move to the next location [51]–[53]. The transition phase from hover to cruise demands a control system capable of maintaining the UAV's position and orientation stability, as sudden changes in flight dynamics can affect data acquisition accuracy [54]–[56]. Additionally, in rescue operations, such as searching for victims of natural disasters or delivering medical supplies to hard-to-reach areas. In these missions, UAVs often have to operate in unstable environments, such as hilly areas, and transition from hover mode while performing detailed searches to cruise mode to reach other areas as quickly as possible. Precision and stability during this transition phase are essential for the UAV to effectively carry out its mission [57]–[59].

Thus, this design presents its own challenges in terms of control, especially during critical transition phases such as landing. In this phase, the transition from forward mode (fixed-wing) to backward mode (multirotor) is very complex because it involves changes in flight dynamics and requires maintaining stability as well as landing accuracy [60]–[62]. To achieve optimal performance, a control system is needed that can accurately and responsively manage changes in rotor configuration. Several control approaches have been proposed to address this challenge, such as PID (Proportional-Integral-Derivative) control [63]–[66], adaptive control [67]–[70], and robust control [64], [71]–[74].

Table II provides a comparison between the three types of control, focusing on the advantages and disadvantages of each control system method that has been implemented in the transition phase of the Tilt Rotor UAV. Currently, research on hybrid UAVs of the Quadcopter Tilting Rotor (QTRA) type is still limited in discussing control systems. Some studies only address performance based on its aerodynamics [75][76]. Optimization analysis in quadcopter mode to elucidate the mass coupling variables between the EPS component analysis module and the mass analysis module is effectively conducted using a multi-objective evolutionary algorithm called NSGA-II to find the full Pareto front for multi-objective problems [77]. Numerical simulations with backstepping control are applied to regulate altitude and position during hybrid transitions [78]. However, further analysis of performance and error values is not explained in detail. Therefore, the optimized Proportional Derivative (PD) control strategy offers a simpler yet effective approach to managing the backward transition during the landing phase of the hybrid quadcopter tilt rotor. This approach focuses on

controlling speed and orientation, which is crucial for maintaining UAV stability during this critical phase. Several studies indicate that PD control, with appropriate parameter adjustments, can yield better performance in reducing oscillations and overshoot, as well as improving system response.

TABLE II. APPLICATION OF TRANSITION PHASE CONTROL SYSTEMS IN HYBRID UAV

Type of Control	Advantages	Disadvantages
PID Control	<ul style="list-style-type: none"> <li>- Simple and easy to implement.</li> <li>- Fast response for position and orientation control.</li> <li>- Widely used in industrial applications and UAVs with stable dynamics.</li> <li>- Parameter tuning (P, I, D) is quite flexible for various types of simple systems.</li> </ul>	<ul style="list-style-type: none"> <li>- Less effective in systems with varying or nonlinear dynamics.</li> <li>- Sensitive to disturbances and noise.</li> <li>- Difficult to manage systems with significant uncertainty or environmental disturbances.</li> <li>- Overshoot and oscillations can occur if parameters are not tuned properly.</li> </ul>
Adaptive Control	<ul style="list-style-type: none"> <li>- Capable of automatically adjusting control parameters according to changes in system conditions.</li> <li>- Effective in handling uncertainty and changes in system dynamics, such as load variations or weather changes.</li> <li>- More flexible for application in non-static or dynamic systems.</li> </ul>	<ul style="list-style-type: none"> <li>- High computational complexity, requiring greater resources.</li> <li>- Slower calculation processes compared to conventional PID control.</li> <li>- More complicated implementation and more susceptible to errors if the model is not accurate.</li> </ul>
Robust Control	<ul style="list-style-type: none"> <li>- Resistant to disturbances and uncertainties in the system.</li> <li>- Effective in maintaining system performance under varying or disruptive environmental conditions.</li> <li>- Better stability in nonlinear conditions and high uncertainty.</li> </ul>	<ul style="list-style-type: none"> <li>- Control design is very complex and requires a good mathematical model.</li> <li>- Requires more complex parameter tuning and is not always easy to apply to all types of systems.</li> <li>- Typically requires heavier computational calculations, making it not always ideal for real-time applications.</li> </ul>

The main objective of this research is to design a backward transition control system for hybrid tilt rotor quadcopters using Proportional Derivative (PD) control during the landing phase. The proposed control system is expected to optimize the transition from fixed-wing mode to quadcopter mode by minimizing oscillations, overshoot, and steady-state errors, as well as enhancing landing accuracy. This research contributes to the development of optimized PD control algorithms for managing backward transitions during the landing phase of hybrid tilt rotor quadcopters. The algorithm is tested through simulations to evaluate its performance. The results of this study are expected to serve as an important reference for further development of Hybrid Quadrotor Tilting Rotor UAVs, particularly in the area of control systems, where research is still limited.

## II. METHOD

### A. Design of the Hybrid Tilt Rotor Quadcopter System

The Hybrid VTOL Quadrotor Tilting Rotor Aircraft UAV is a model designed to travel in fixed-wing mode and land vertically in rotary wing or quadcopter mode.

Fig. 1 shows the Hybrid QTRA model used in the research, separating the actuator controller from the mechanism [79]. The model also includes the selection of the controller mode, allowing for the choice between the transition mode controller and the quadcopter mode controller, which can be selected for use [37]. The following is the design of the Hybrid QTRA system that has been developed.

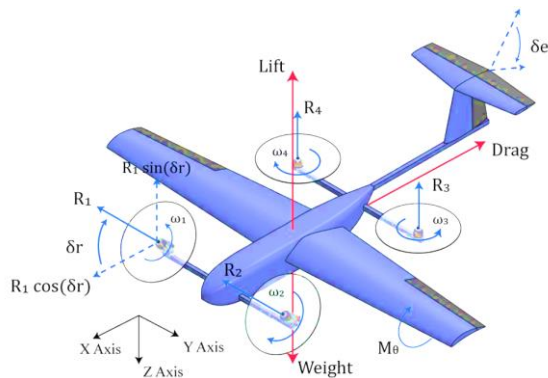


Fig. 1. Hybrid VTOL QTRA

The input signal consists of a trajectory waypoint, and the control signal then enters the mode selector as a decision and mixer, where there are two conditions to choose from: FW for fixed-wing and QR for quadrotor. In Fig. 2, the system's mode selector block compares the UAV's actual position with the target waypoint, and the selector instructs the UAV to choose the appropriate mode. The reference signal from the mode selector is then sent to three different blocks: the FW controller, the QR controller, and the tiltrotor algorithm. In the tiltrotor algorithm, when the block receives an FW signal, the tiltrotor condition will produce a target tilt angle of  $0^\circ$ , if it receives a QR signal, it will produce a target tilt angle of

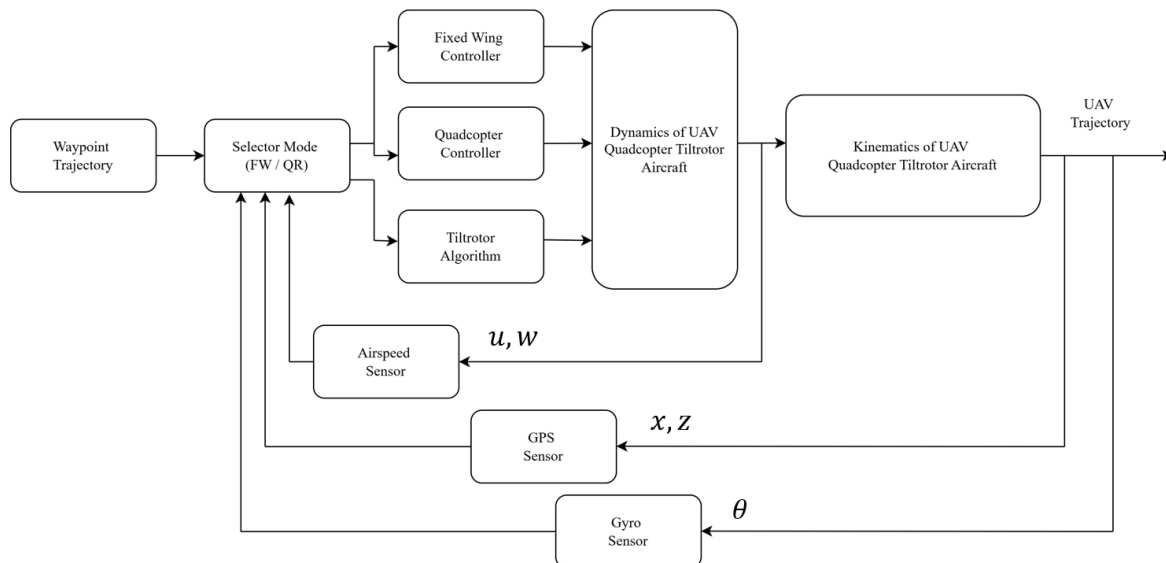


Fig. 2. Block diagram of the plant in the hybrid VTOL QTRA UAV system

$90^\circ$ . Both controllers will generate reference thrust and moment values, which will serve as manipulation variables, and then enter the UAV dynamics model. There are five manipulation variables in the hybrid QTRA system: the thrust force from the two front rotors  $R_1$  and  $R_2$  as  $u_1$ , the two rear rotors  $R_3$  and  $R_4$  as  $u_2$ , the deflection angle of the elevator  $\delta_e$  as  $u_3$ , the additional pitch moment angle in quadcopter mode  $M_\theta$  as  $u_4$ , and the tilting rotor angle  $\delta_r$  which is modeled by adding a servo motor to the system, allowing for a change in direction of the thrust from the front rotors as  $u_5$ . For the elevator actuator angle, the degree is limited to  $15^\circ$  upward and  $15^\circ$  downward. Meanwhile, for the tilt rotor actuator angle, the lower limit is set to  $0^\circ$ , indicating that the tilt angle of the two front rotors is in a horizontal position functioning in fixed-wing mode, while the upper limit is set to  $90^\circ$ , indicating that the tilt angle of the two front rotors points vertically functioning in quadcopter mode. In the simulation, the rotational speed of the rotors, denoted as  $\omega_1$  to  $\omega_4$ , is limited to a speed of 5000 RPM based on the specifications of the Emax MT3515 650kv motor. The pitch angle is modeled to ensure that it does not exceed a limit of  $12^\circ$ , as the UAV has a stall angle of  $12^\circ$ .

### B. Mathematical Model of UAV Dynamics

In the simulation, several specification parameters are needed as constant inputs in the vehicle model. According to Table III, these parameters are intended to facilitate calculations and simulations for the QTRA UAV.

TABLE III. QTRA UAV SPECIFICATION PARAMETERS

No	Variable	Value	Unit
1	Massa (m)	6	Kg
2	Area of Fixed Wing (S)	0.55	m <sup>2</sup>
3	Mean Aerodynamic Chord ( $\bar{c}$ )	0.282	m
4	Wingspan (l)	2	m
5	Moment of Inertia on y axis ( $I_{yy}$ )	0.7893	Kg.m <sup>2</sup>
6	Thrust Koefisien ( $K_T$ )	0.1142	Kg.m
7	Air Density ( $\rho$ )	12.133	Kg/m <sup>3</sup>
8	Rotor Positions 1 and 2	0.25	m
9	Rotor Positions 3 and 4	-0.5	m
10	Gravity	9.8	m/s <sup>2</sup>

The dynamics of translational velocity along the x-axis is obtained from the following equation (1):

$$\begin{aligned} \dot{u} = & -qw + \frac{1}{m} (\{ \{ CL_0 + C_{L\alpha}\alpha + C_{Lq} \frac{q\bar{c}}{2V_\alpha} + \\ & C_{L\delta_e} \delta_e \} \sin \alpha - (C_{D_{min}} + K \{ C_L - C_{L,C_{D_{min}}} \}^2 + \\ & C_{D_{\delta_e}} |\delta_e|) \cos \alpha \} \frac{1}{2} \rho V_\alpha^2 S) + \{- \sin \theta [mg] \} + \\ & \{ \cos \delta [K_T \sum_{i=1}^4 \omega_i^2] \} \end{aligned} \quad (1)$$

The translational velocity along the z-axis, denoted as the variable  $\dot{w}$ , is as follows:

$$\begin{aligned} \dot{w} = & qu + \frac{1}{m} (\{ \{ - (CL_0 + C_{L\alpha}\alpha + C_{Lq} \frac{q\bar{c}}{2V_\alpha} + \\ & C_{L\delta_e} \delta_e) \cos \alpha - (C_{D_{min}} + K \{ C_L - C_{L,C_{D_{min}}} \}^2 + \\ & C_{D_{\delta_e}} |\delta_e|) \sin \alpha \} \frac{1}{2} \rho V_\alpha^2 S \} + \{ \cos \theta [mg] \} + \\ & \{ \sin \delta [K_T \sum_{i=1}^4 \omega_i^2] \} \end{aligned} \quad (2)$$

The calculation of the moments acting on the aircraft includes the moment generated by the thrust on the aircraft as  $M_r(total)$  along with the aerodynamic moment occurring on the aircraft as  $M_a$ . Thus, the total moment in the body frame is represented as  $M_b$  in the equation (3).

$$\begin{aligned} M_b = & M_r(total) + M_a \\ = & (0.25 \times u_{12} \sin \delta \\ & - 0.5 \times u_{34} \sin 90^\circ) + Q C_L S \bar{c} \end{aligned} \quad (3)$$

In the aerodynamic frame, as shown in Fig. 3, there are additional variables represented by  $\alpha$  and  $\beta$ , where  $\alpha$  is denoted as the angle of attack, which is the angle of incidence occurring at the aircraft's wing in the longitudinal direction between axis  $X_A$  and axis  $X_B$ . Meanwhile,  $\beta$  is the angle between axis  $X_A$  and the wind speed  $V$  occurring in the lateral direction of the aircraft, where the lateral axis of the aircraft is depicted as the X and Y plane in the body frame with a red rectangle. The speed of the UAV, or UAV airspeed, is defined as the resultant non-dimensional speed from two directions of the UAV, formulated as  $V_\alpha$  in the following equation.

$$V_\alpha = \sqrt{u^2 + w^2} \quad (4)$$

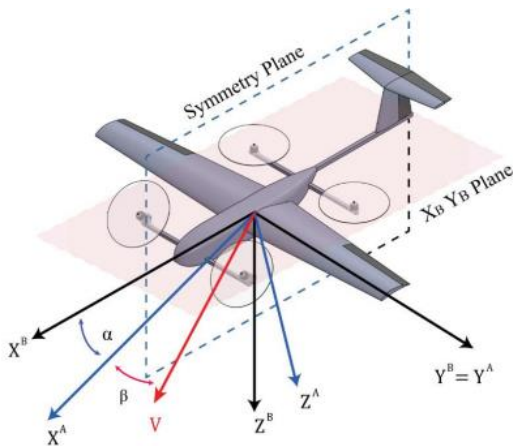


Fig. 3. Aerodynamic frame of the hybrid VTOL QTRA UAV system

In conditioning the resultant of two velocities in different directions, the square of each velocity is needed, and then the sum of the two velocities is given a square root to produce the

final resultant speed. The angle separating the two frames is written as angle  $\alpha$ . Using trigonometric laws, the rotation between angle  $X_B$  in the body frame and  $X_A$  in the aerodynamic frame is obtained as follows:

$$X_A = X_B \cos \alpha + Z_B \sin \alpha \quad (5)$$

$$Y_A = Y_B \quad (6)$$

$$Z_A = X_B (-\sin \alpha) + Z_B \cos \alpha \quad (7)$$

$$R_b^a = \begin{pmatrix} X_A \\ Y_A \\ Z_A \end{pmatrix} = \begin{pmatrix} \cos \alpha & 0 & \sin \alpha \\ 0 & 1 & 0 \\ -\sin \alpha & 0 & \cos \alpha \end{pmatrix} \begin{pmatrix} X_B \\ Y_B \\ Z_B \end{pmatrix} \quad (8)$$

In analyzing the transformation displacement from the vehicle frame to the body frame, the rotation matrix of the aircraft from the vehicle to the body is obtained. Thus, the equation is derived as follows:

$$\begin{aligned} \mathcal{R}_v^b(\phi, \theta, \psi) &= \mathcal{R}_{v2}^b(\phi) \mathcal{R}_{v1}^{v2}(\theta) \mathcal{R}_v^{v1}(\psi) \\ \mathcal{R}_v^b(\phi, \theta, \psi) &= \begin{pmatrix} C_\theta C_\psi & C_\theta S_\psi & -S_\psi \\ S_\phi S_\theta C_\psi - C_\phi S_\psi & S_\phi S_\theta S_\psi + C_\phi C_\psi & S_\phi C_\theta \\ C_\phi S_\theta C_\psi + S_\phi S_\psi & C_\phi S_\theta S_\psi - S_\phi C_\psi & C_\phi C_\theta \end{pmatrix} \end{aligned} \quad (9)$$

Since the system has a degree of freedom of 3 (Degree of Freedom, DOF), it is formulated that the system can have 6 states, while the controller input in the system is represented by 5 inputs.

$$\dot{x}(t) = (\dot{u} \ \dot{w} \ \dot{q} \ \dot{\theta} \ \dot{x} \ \dot{z})^T \quad (10)$$

$$u(t) = (u_1 \ u_2 \ u_3 \ u_4 \ u_5)^T \quad (11)$$

### C. Control System

In controlling several control variables on the UAV, such as ailerons, elevators, rudders, and rotor speed, both linear and nonlinear controllers can be implemented. Some examples of applying linear controllers on UAVs include the use of Proportional Integral Derivative (PID) controllers, eigenvalue assignment, robust control, model predictive control, and gain scheduling. Meanwhile, some nonlinear controllers that can be implemented include Backstepping Proportional Derivative, Sliding Mode, and Lyapunov.

In the research conducted, a nonlinear control was used with a Proportional-Derivative (PD) controller without employing the backstepping method to control the transition of the UAV. In Fig. 4, there are three modes that can be provided by the backward transition algorithm, namely cruising mode using the fixed wing, transition mode, and landing mode using the quadcopter.

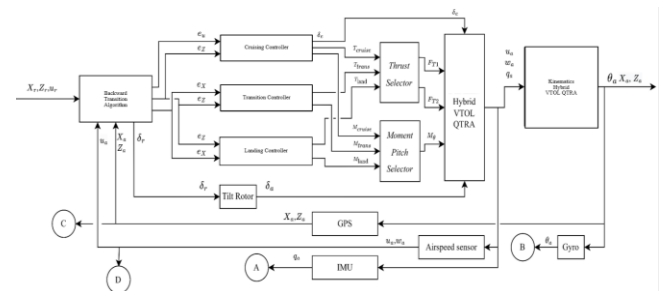


Fig. 4. Control block diagram of hybrid VTOL QTRA

The fixed wing controller block in Fig. 5 can only be used when the backward transition algorithm determines that the mode used by the UAV is cruising mode with fixed wing. The pitch comparison will be controlled again using the Proportional Derivative (PD) controller, which generates a reference angular velocity value for pitch, denoted as  $q_r$  which is then compared with the actual angular velocity value  $q_a$ . The comparison result from both blocks will produce an output as the deflection angle for the elevator, where the elevator movement is restricted to a range of  $15^\circ$  to  $-15^\circ$ .

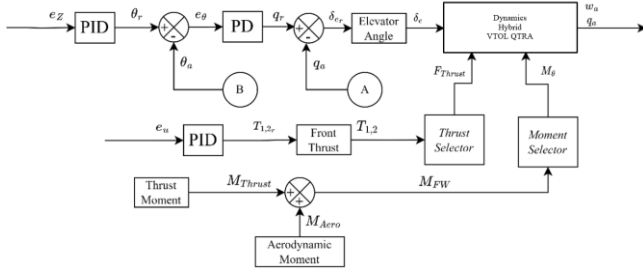


Fig. 5. Cruising controller with fixed-wing mode

The transition controller model is further explained in Fig. 6. Immediately after the aircraft receives the command to perform a transition, the transition controller will activate by obtaining inputs as the error value on the Z-axis, denoted as  $e_z$  and the error on the X-axis, denoted as  $e_x$ . The error value on the X-axis  $e_x$ , will be controlled using the PD controller, which generates a reference pitch value  $\theta_x$ . The next controller is the landing or VTOL controller, represented in Fig. 7. This controller again requires input error values on the X-axis as  $e_x$  along with the error value on the Z-axis as  $e_z$  to land the UAV system. The X setpoint used has the same value as when the UAV undergoes the transition condition, with the goal that the UAV does not experience a change in X position during landing, while maintaining the pitch moment of the UAV to remain stable. The input setpoint value that differs in the landing controller from the previous transition controller is the height input, where it is targeted that the UAV can achieve a height of 0 meters.

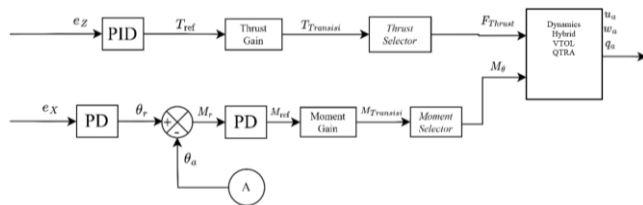


Fig. 6. Transition controller with quadcopter mode

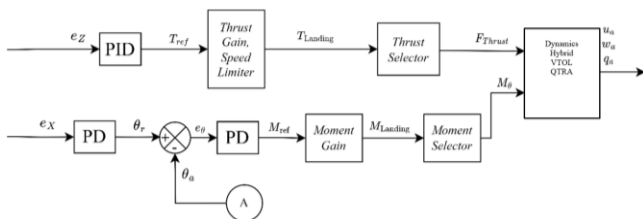


Fig. 7. Landing controller with quadcopter mode

The mode will determine which controller will be used in the system among the three main controller blocks in Fig. 4. The backward transition algorithm block also determines the

tilting angle of the rotor in changing the thrust angle of the two front rotors. The first controller in the system is the cruising controller, the second controller is the transition controller, and the third controller is the landing controller.

### III. RESULTS AND DISCUSSION

The modeling of the control system is carried out by incorporating mathematical equations into the MATLAB Simulink software. The elaboration of the state differential equations in the system is performed using the expand function in MATLAB, making the linearization process easily conducted with the Jacobian algorithm. Below are the differential equations in matrices A and B that will be used in the control system.

$$\dot{X} = AX + BU$$

$$= \begin{pmatrix} X_u & X_w & X_q & -g \cos \theta & 0 & 0 \\ Z_u & Z_w & Z_q & -g \sin \theta & 0 & 0 \\ M_u & M_w & M_q & 0 & 0 & 0 \\ 0 & 0 & 1 & 0 & 0 & 0 \\ \cos(\theta) & \sin(\theta) & 0 & X_{dt} & 0 & 0 \\ -\sin(\theta) & \cos(\theta) & 0 & Z_{dt} & 0 & 0 \end{pmatrix} \begin{pmatrix} \dot{u} \\ \dot{w} \\ \dot{q} \\ \dot{\theta} \\ \dot{x} \\ \dot{z} \end{pmatrix} \quad (12)$$

$$+ \begin{pmatrix} X_{u_1} & 0 & X_{u_3} & 0 & X_{u_5} \\ Z_{u_1} & -0.3333 & Z_{u_3} & 0 & Z_{u_5} \\ M_{u_1} & -1.2670 & M_{u_3} & 1.2670 & M_{u_5} \\ 0 & 0 & 0 & 0 & 0 \\ 0 & 0 & 0 & 0 & 0 \\ 0 & 0 & 0 & 0 & 0 \end{pmatrix} \begin{pmatrix} u_1 \\ u_2 \\ u_3 \\ u_4 \\ u_5 \end{pmatrix}$$

The Backward Transition algorithm block also has inputs C and D, which represent the actual position values on the x-axis as  $x_a$ , the actual position on the z-axis as  $z_a$ , and the actual horizontal velocity as  $u_a$ .

The comparison of reference and actual values, shown in Fig. 8, will result in error values, where  $e_x$  is the error for the x setpoint,  $e_z$  is the error for the z setpoint, and  $e_u$  is the error for the horizontal speed setpoint. The reference setpoint values are as follows  $X_r$  is 3000 during cruising and 3120 during hovering and landing;  $Z_r$  is 100 during cruising and hovering, and 0 during landing.  $U_r$  is 30 during cruising and 0 during hovering and landing. Parameter tuning is used to achieve maximum performance by controlling the required response time and robustness of the controller. Fig. 9 shows one of the position X controller systems during the transition, which is robust and has a quick response time with a proportional gain (P) of 27626.55 and a derivative gain (D) of 1578.49. Thus, the gain values for the control system are presented in Table IV.

TABLE IV. UAV QTRA CONTROLLER ENHANCEMENT

Controller Variable	Loop	Gain	Mode		
			Cruise	Transisi	VTOL
Controller X	Outer	P	-	0.001	0.001
		D	-	-0.076	-0.076
	Inner	P	-	27627.2	27627.2
		D	-	1578.53	1578.5
Controller Y	Outer	P	0.047	-0.465	28.613
		I	0.001	-0.081	-
		D	0.32	-0.397	12.903
	Inner	P	146.05	-	-
		D	12.948	-	-
		I	29621	-	-
Controller U	Outer	P	29621	-	-
		I	54355155	-	-
		D	0.025	-	-

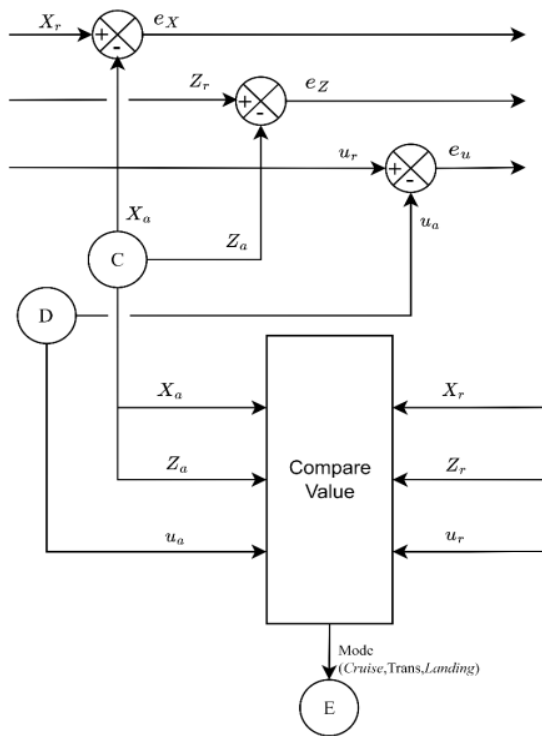


Fig. 8. Backward transition algorithm

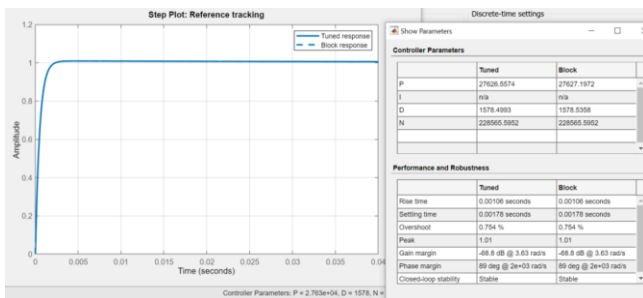


Fig. 9. Tuning the PD controller during the transition process

The first closed-loop test simulation was conducted in cruising mode, where the aircraft was positioned at an altitude of 70 m above the ground and was increased to 100 m. The altitude increase of the aircraft was controlled using the elevator at the tail to reach the setpoint at an altitude of 100 m.

The response shown in Fig. 10 indicates that the UAV first increased its altitude to 106 m before reaching the target set point of 100 m. The UAV experienced fluctuations with an overshoot during PID control, as the elevator continuously worked to maintain altitude stability at 100 m. In steady conditions, the altitude error was measured at 0.41 m. This can be improved by adjusting the controller gains to optimize system response. In testing the increase in distance along the x-axis, the response graph demonstrated a stable increase in distance x corresponding to the time function. Fig. 11 shows the close-loop transition test, where the UAV is targeted to stabilize its position at specific set points for x and z. In the transition mode of the UAV system, the aircraft, starting from an initial altitude of 100.41 m, aims to establish its position at 100 m. It can be observed that the altitude change during the transition condition has a relatively fast response, with a settling time of less than 20 seconds. Meanwhile, for the

control of the x position, the data indicates that the position control has a relatively longer settling time of 59 seconds. This is due to the fact that the x position controller on the UAV in quadcopter mode has two different controllers, which results in the UAV requiring longer control times. The third closed-loop test was conducted in landing mode, where the aircraft needed to control its position at 3120 m, with a height set point of 0 m to ensure a successful landing. This closed-loop test can be seen in Fig. 12. The aircraft decelerates its vertical speed as it approaches the 0 m set point. The VTOL controller in this system uses PD controller gains combined with the thrust from both the front and rear, allowing the UAV to reach the desired altitude. Meanwhile, to maintain stability in the x position, the same type of controller used in the transition phase is employed, affecting the moment on the UAV to prevent any shift in the x position.

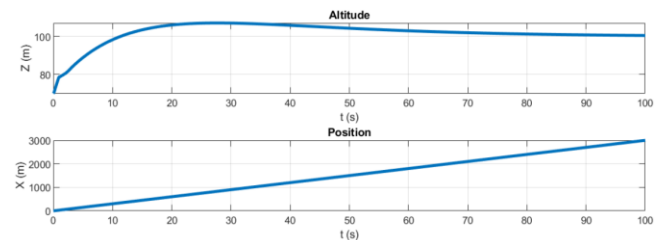


Fig. 10. Results of the cruising system testing

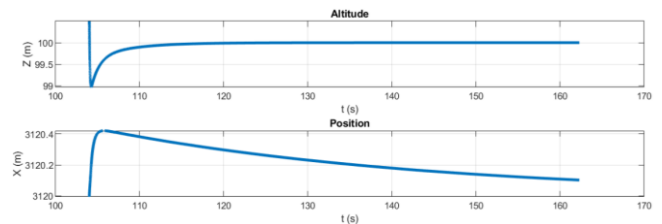


Fig. 11. Results of the transition system testing

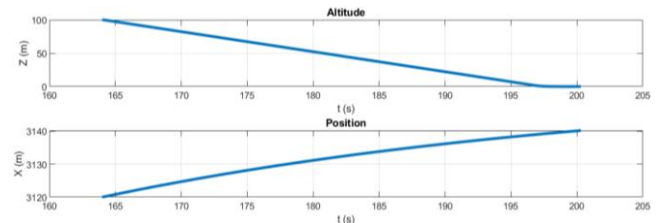


Fig. 12. Results of the landing system testing

By using the VTOL transition control algorithm from cruise mode with fixed wings to hover and then proceeding to the landing process, the trajectory tracking of the system is shown in Fig. 13. During cruising in fixed wing mode, the initial z position is set at a height of 70 m, and the travel distance is set to 0 m, stabilizing the trim condition of the fixed wing aircraft. The UAV performs a pitch maneuver to reach the setpoint at a height of 100 m on the z-axis. The UAV then travels a distance of 4800 m along the x-axis and lands at that coordinate. During the landing process, the UAV is targeted to maintain its position at a distance of 3120 m along the x-axis while reaching the setpoint at a height of 0 m on the z-axis. However, during the position control when landing, the UAV experienced a position shift of 20 m, thus failing to achieve stability in the x position during landing.

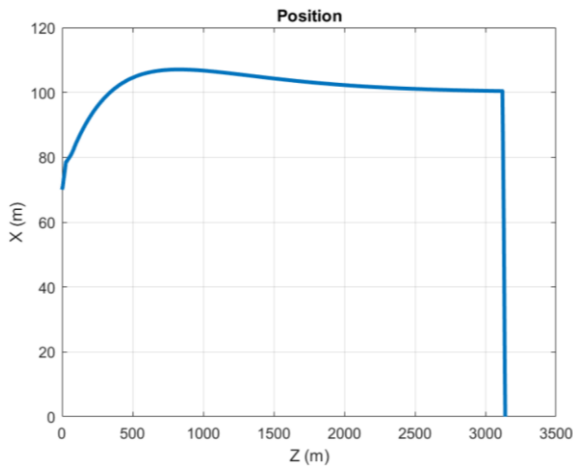


Fig. 13. Trajectory results of hybrid VTOL QTRA aircraft

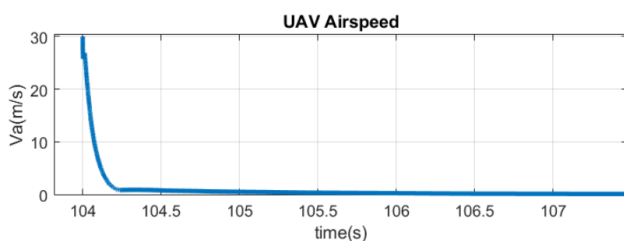
Performance testing was conducted for each different condition, with each mode having its own controller. The first performance test obtained data for  $z$  during cruising as shown in Fig. 10, where the response to the setpoint of 100 m on the  $z$ -axis while cruising in fixed wing mode resulted in a system error of 5%, with a settling time of 100 seconds. The input to this controller can be said to meet the criteria of a control system, where the overshoot is a maximum of 5%. The following Table V presents the performance results for each test in every mode.

TABLE V. SYSTEM PERFORMANCE TEST RESULTS

State	Settling Time (s)	Steady State Error	Max Overshoot
Z (cruise)	100	0.4 m	5%
Z (transition)	57	0 m	1%
Z (landing)	35	0 m	0%
X (transition)	57	0.1 m	0.4%
X (landing)	35	20 m	20%

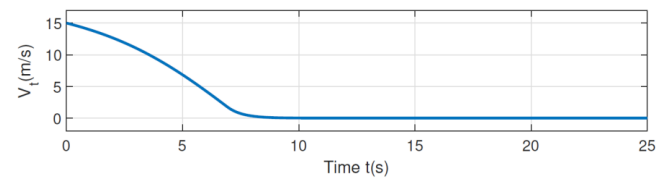
From this study, the airspeed response  $V_a$  was obtained using the equation (4).

The data in Fig. 14 obtained shows that the airspeed during the transition in this study has a response time and settling time that is relatively faster compared to previous research [80].

Fig. 14. Response of airspeed  $V_a$  over time

The rise time in this study was achieved in 0.5 seconds, while in previous research, it took 5 seconds. The settling time in this study was found to be 1.5 seconds, compared to 7 seconds in previous research. The results in Fig. 15 also demonstrate that the transition process did not cause any overshoot from the target airspeed of 0 m/s. A drawback of the simulation results in this study is that the airspeed during

the transition condition is less smooth; however, it still managed to reach the same setpoint.

Fig. 15. The response of airspeed  $V_t$  over time [80]

#### IV. CONCLUSION

The landing process system has been designed for the UAV Hybrid VTOL QTRA with PID and PD controllers to manage the transition from cruising mode to landing. The transition mechanism changes the tilting rotor manipulation variable from  $0^\circ$  to  $90^\circ$ , increasing the lift force of the UAV from the rotors to compensate for the aerodynamic lift, and adjusts the  $x$  position setpoint in quadcopter mode by modifying the moment on the UAV. The response of the Hybrid VTOL QTRA system is robust, although it has a relatively long settling time. The performance response results of the UAV indicate a response time of 57 seconds, with an overshoot of 1% in the  $z$  position and 0.4% in the  $x$  position. The steady-state error in the system is recorded as 0 m for altitude  $z$  and 0.1 m for position  $x$ . Future research could introduce variations in the speed of the rotor tilt angle changes and cruising, as well as variations in controller gain using diverse tuning methods to achieve optimal performance during the UAV transition process.

#### ACKNOWLEDGMENT

The author is very grateful for the funding and facilities provided by the Department of Physical Engineering on the basis of the research No: 987/PKS/ITS/2024.

#### REFERENCES

- [1] C. Li, Y. Gan, Y. Zhang, and Y. Luo, "A Cooperative Computation Offloading Strategy With On-Demand Deployment of Multi-UAVs in UAV-Aided Mobile Edge Computing," *IEEE Trans. Netw. Serv. Manag.*, vol. 21, no. 2, pp. 2095–2110, 2024, doi: 10.1109/TNSM.2023.3332899.
- [2] R. M. Rolly, P. Malarvezhi, and T. D. Lagkas, "Unmanned aerial vehicles: Applications, techniques, and challenges as aerial base stations," *Int. J. Distrib. Sens. Networks*, vol. 18, no. 9, 2022, doi: 10.1177/15501329221123933.
- [3] G. Lin, H. Li, C. K. Ahn, and D. Yao, "Event-Based Finite-Time Neural Control for Human-in-the-Loop UAV Attitude Systems," *IEEE Trans. Neural Networks Learn. Syst.*, vol. 34, no. 12, pp. 10387–10397, 2023, doi: 10.1109/TNNLS.2022.3166531.
- [4] R. Akter, M. Golam, V. S. Doan, J. M. Lee, and D. S. Kim, "IoMT-Net: Blockchain-Integrated Unauthorized UAV Localization Using Lightweight Convolution Neural Network for Internet of Military Things," *IEEE Internet Things J.*, vol. 10, no. 8, pp. 6634–6651, 2023, doi: 10.1109/JIOT.2022.3176310.
- [5] M. Ciopcia and C. Szczepański, "Quad-Tiltrotor—modelling and control," *J. Mar. Eng. Technol.*, vol. 16, no. 4, pp. 331–336, 2018, doi: 10.1080/20464177.2017.1388068.
- [6] J. Chen, C. Du, Y. Zhang, P. Han, and W. Wei, "A Clustering-Based Coverage Path Planning Method for Autonomous Heterogeneous UAVs," *IEEE Trans. Intell. Transp. Syst.*, vol. 23, no. 12, pp. 25546–25556, 2022, doi: 10.1109/TITS.2021.3066240.
- [7] D. K. Jain, Y. Li, M. J. Er, Q. Xin, D. Gupta, and K. Shankar, "Enabling Unmanned Aerial Vehicle Borne Secure Communication With Classification Framework for Industry 5.0," *IEEE Trans. Ind.*

- Informatics*, vol. 18, no. 8, pp. 5477–5484, 2022, doi: 10.1109/TII.2021.3125732.
- [8] A. Fotouhi *et al.*, “Survey on UAV Cellular Communications: Practical Aspects, Standardization Advancements, Regulation, and Security Challenges,” *IEEE Commun. Surv. Tutorials*, vol. 21, no. 4, pp. 3417–3442, 2019, doi: 10.1109/COMST.2019.2906228.
- [9] A. P. Cohen, S. A. Shaheen, and E. M. Farrar, “Urban Air Mobility: History, Ecosystem, Market Potential, and Challenges,” *IEEE Trans. Intell. Transp. Syst.*, vol. 22, no. 9, pp. 6074–6087, 2021, doi: 10.1109/TITS.2021.3082767.
- [10] S. Aggarwal, N. Kumar, and S. Tanwar, “Blockchain-envisioned UAV communication using 6G networks: Open issues, use cases, and future directions,” *IEEE Internet Things J.*, vol. 8, no. 7, pp. 5416–5441, 2021, doi: 10.1109/JIOT.2020.3020819.
- [11] S. A. H. Mohsan, N. Q. H. Othman, Y. Li, M. H. Alsharif, and M. A. Khan, “Unmanned aerial vehicles (UAVs): practical aspects, applications, open challenges, security issues, and future trends,” *Intell. Serv. Robot.*, vol. 16, no. 1, pp. 109–137, 2023, doi: 10.1007/s11370-022-00452-4.
- [12] A. Buffi, A. Motroni, P. Nepa, B. Tellini, and R. Cioni, “A SAR-Based Measurement Method for Passive-Tag Positioning with a Flying UHF-RFID Reader,” *IEEE Trans. Instrum. Meas.*, vol. 68, no. 3, pp. 845–853, 2019, doi: 10.1109/TIM.2018.2857045.
- [13] A. N. Wilson, A. Kumar, A. Jha, and L. R. Ceneramaddi, “Embedded Sensors, Communication Technologies, Computing Platforms and Machine Learning for UAVs: A Review,” *IEEE Sens. J.*, vol. 22, no. 3, pp. 1807–1826, 2022, doi: 10.1109/JSEN.2021.3139124.
- [14] M. A. O. Rabah, H. Drid, M. Rahouti, and N. Lazaar, *Empowering UAV Communications with AI-Assisted Software-Defined Networks: A Review on Performance, Security, and Efficiency*, vol. 32, no. 4, 2024, doi: 10.1007/s10922-024-09866-0.
- [15] C. Chen *et al.*, “YOLO-Based UAV Technology: A Review of the Research and Its Applications,” *Drones*, vol. 7, no. 3, 2023, doi: 10.3390/drones7030190.
- [16] M. Hassanalian and A. Abdelkefi, “Classifications, applications, and design challenges of drones: A review,” *Prog. Aerosp. Sci.*, vol. 91, pp. 99–131, 2017, doi: 10.1016/j.paerosci.2017.04.003.
- [17] E. Tal, G. Ryou, and S. Karaman, “Aerobatic Trajectory Generation for a VTOL Fixed-Wing Aircraft Using Differential Flatness,” *IEEE Trans. Robot.*, vol. 39, no. 6, pp. 4805–4819, 2023, doi: 10.1109/TRO.2023.3301312.
- [18] P. Poksawat, L. Wang, and A. Mohamed, “Gain Scheduled Attitude Control of Fixed-Wing UAV with Automatic Controller Tuning,” *IEEE Trans. Control Syst. Technol.*, vol. 26, no. 4, pp. 1192–1203, 2018, doi: 10.1109/TCST.2017.2709274.
- [19] K. Yamaguchi and S. Hara, “On Structural Parameter Optimization Method for Quad Tilt-Wing UAV Based on Indirect Size Estimation of Domain of Attraction,” *IEEE Access*, vol. 10, pp. 1678–1687, 2022, doi: 10.1109/ACCESS.2021.3139156.
- [20] D. Brescianini and R. D’Andrea, “Tilt-Prioritized Quadcopter Attitude Control,” *IEEE Trans. Control Syst. Technol.*, vol. 28, no. 2, pp. 376–387, 2020, doi: 10.1109/TCST.2018.2873224.
- [21] S. A. H. Mohsan, M. A. Khan, F. Noor, I. Ullah, and M. H. Alsharif, “Towards the Unmanned Aerial Vehicles (UAVs): A Comprehensive Review,” *Drones*, vol. 6, no. 6, p. 147, 2022.
- [22] C. Lee, S. Kim, and B. Chu, “A Survey: Flight Mechanism and Mechanical Structure of the UAV,” *Int. J. Precis. Eng. Manuf.*, vol. 22, no. 4, pp. 719–743, 2021, doi: 10.1007/s12541-021-00489-y.
- [23] P. S. Ramesh and J. V. Muruga Lal Jeyan, “Comparative Analysis of Fixed-Wing, Rotary-Wing and Hybrid Mini Unmanned Aircraft Systems (UAS) from the Applications Perspective,” *INCAS Bull.*, vol. 14, no. 1, pp. 137–151, 2022, doi: 10.13111/2066-8201.2022.14.1.12.
- [24] E. J. J. Smeur, M. Bronz, and G. C. H. E. de Croon, “Incremental control and guidance of hybrid aircraft applied to a tailsitter unmanned air vehicle,” *J. Guid. Control. Dyn.*, vol. 43, no. 2, pp. 274–287, 2020, doi: 10.2514/1.G004520.
- [25] Z. Wang, R. Zu, D. Duan, and J. Li, “Tuning of ADRC for QTR in Transition Process Based on NBPO Hybrid Algorithm,” *IEEE Access*, vol. 7, pp. 177219–177240, 2019, doi: 10.1109/ACCESS.2019.2957318.
- [26] S. Panigrahi, Y. S. S. Krishna, and A. Thondiyath, “Design, analysis, and testing of a hybrid vtol tilt-rotor uav for increased endurance,” *Sensors*, vol. 21, no. 18, pp. 1–21, 2021, doi: 10.3390/s21185987.
- [27] C. Zeng, R. Abnous, K. Gabani, S. Chowdhury, and V. Maldonado, “A new tilt-arm transitioning unmanned aerial vehicle: Introduction and conceptual design,” *Aerosp. Sci. Technol.*, vol. 99, p. 105755, 2020, doi: 10.1016/j.ast.2020.105755.
- [28] H. Zhao, B. Wang, Y. Shen, Y. Zhang, N. Li, and Z. Gao, “Development of Multimode Flight Transition Strategy for Tilt-Rotor VTOL UAVs,” *Drones*, vol. 7, no. 9, pp. 1–19, 2023, doi: 10.3390/drones7090580.
- [29] A. S. Saeed, A. B. Younes, C. Cai, and G. Cai, “A survey of hybrid Unmanned Aerial Vehicles,” *Prog. Aerosp. Sci.*, vol. 98, pp. 91–105, 2018, doi: 10.1016/j.paerosci.2018.03.007.
- [30] D. Duan, Z. Wang, Q. Wang, and J. Li, “Research on integrated optimization design method of high-efficiency motor propeller system for UAVs with multi-states,” *IEEE Access*, vol. 8, pp. 165432–165443, 2020, doi: 10.1109/ACCESS.2020.3014411.
- [31] C. Chen, J. Zhang, D. Zhang, and L. Shen, “Control and flight test of a tilt-rotor unmanned aerial vehicle,” *Int. J. Adv. Robot. Syst.*, vol. 14, no. 1, pp. 1–12, 2017, doi: 10.1177/1729881416678141.
- [32] N. Mohammadi, M. Tayefi, and M. Zhu, “Nonlinear modeling and designing transition flight control scenarios for a dual thrust hybrid UAV,” *Int. J. Intell. Robot. Appl.*, vol. 8, no. 3, pp. 525–545, 2024, doi: 10.1007/s41315-024-00354-x.
- [33] J. ZHONG and C. WANG, “Transition characteristics for a small tailsitter unmanned aerial vehicle,” *Chinese J. Aeronaut.*, vol. 34, no. 10, pp. 220–236, 2021, doi: 10.1016/j.cja.2020.12.021.
- [34] R. Yang, C. Du, Y. Zheng, H. Gao, Y. Wu, and T. Fang, “PPO-Based Attitude Controller Design for a Tilt Rotor UAV in Transition Process,” *Drones*, vol. 7, no. 8, 2023, doi: 10.3390/drones7080499.
- [35] B. Li, J. Sun, W. Zhou, C. Y. Wen, K. H. Low, and C. K. Chen, “Transition Optimization for a VTOL Tail-Sitter UAV,” *IEEE/ASME Trans. Mechatronics*, vol. 25, no. 5, pp. 2534–2545, 2020, doi: 10.1109/TMECH.2020.2983255.
- [36] N. LIU, Z. CAI, Y. WANG, and J. ZHAO, “Fast level-flight to hover mode transition and altitude control in tiltrotor’s landing operation,” *Chinese J. Aeronaut.*, vol. 34, no. 1, pp. 181–193, 2021, doi: 10.1016/j.cja.2020.09.041.
- [37] Z. Kong and Q. Lu, “Mathematical Modeling and Modal Switching Control of a Novel Tiltrotor UAV,” *J. Robot.*, vol. 2018, pp. 12–15, 2018, doi: 10.1155/2018/8641731.
- [38] A. Misra *et al.*, “A Review on Vertical Take-Off and Landing (VTOL) Tilt-Rotor and Tilt Wing Unmanned Aerial Vehicles (UAVs),” *J. Eng.*, vol. 2022, pp. 1–27, 2022, doi: 10.1155/2022/1803638.
- [39] S. Du and Y. Zha, “Numerical simulation of the transition flight aerodynamics of cross - shaped quad - tiltrotor UAV,” *Sci. Rep.*, pp. 1–12, 2024, doi: 10.1038/s41598-024-68927-1.
- [40] Z. Lin, B. Yan, T. Zhang, S. Li, Z. Meng, and S. Liu, “Multi-Level Switching Control Scheme for Folding Wing VTOL UAV Based on Dynamic Allocation,” *Drones*, vol. 8, no. 7, pp. 1–22, 2024, doi: 10.3390/drones8070303.
- [41] Q. Huang, G. He, J. Jia, Z. Hong, and F. Yu, “Numerical Simulation on Aerodynamic Characteristics of Transition Section of Tilt-Wing Aircraft,” *Aerospace*, vol. 11, no. 4, p. 283, 2024.
- [42] C. Kikumoto, T. Urakubo, K. Sabe, and Y. Hazama, “Back-Transition Control With Large Deceleration for a Dual Propulsion VTOL UAV Based on Its Maneuverability,” *IEEE Robot. Autom. Lett.*, vol. 7, no. 4, pp. 11697–11704, 2022, doi: 10.1109/LRA.2022.3205450.
- [43] A. N. De Lucena, B. M. F. Da Silva, and L. M. G. Gonçalves, “Double Hybrid Tailsitter Unmanned Aerial Vehicle With Vertical Takeoff and Landing,” in *IEEE Access*, vol. 10, pp. 32938–32953, 2022, doi: 10.1109/ACCESS.2022.3161490.
- [44] R. Zhao *et al.*, “Analysis, optimization, and testing of a tilt-body aircraft,” *Aerosp. Sci. Technol.*, vol. 154, no. July, 2024, doi: 10.1016/j.ast.2024.109385.
- [45] M. Sajid, H. Mittal, S. Pare, and M. Prasad, “Routing and scheduling optimization for UAV assisted delivery system: A hybrid approach,” *Appl. Soft Comput.*, vol. 126, p. 109225, 2022, doi: 10.1016/j.asoc.2022.109225.



- [46] R. She and Y. Ouyang, "Efficiency of UAV-based last-mile delivery under congestion in low-altitude air," *Transp. Res. Part C Emerg. Technol.*, vol. 122, p. 102878, 2021, doi: 10.1016/j.trc.2020.102878.
- [47] E. Tal and S. Karaman, "Global Incremental Flight Control for Agile Maneuvering of a Tailsitter Flying Wing," *J. Guid. Control. Dyn.*, vol. 45, no. 12, pp. 2332–2349, 2022, doi: 10.2514/1.G006645.
- [48] J. B. Willis and R. W. Beard, "Pitch and Thrust Allocation for Full-Flight-Regime Control of Winged eVTOL UAVs," *IEEE Control Syst. Lett.*, vol. 6, pp. 1058–1063, 2022, doi: 10.1109/LCSYS.2021.3089130.
- [49] L. Bauersfeld, L. Spannagl, G. Ducard, and C. Onder, "MPC Flight Control for a Tilt-Rotor VTOL Aircraft," *IEEE Trans. Aerosp. Electron. Syst.*, vol. 57, no. 4, pp. 2395–2409, 2021, doi: 10.1109/TAES.2021.3061819.
- [50] S. M. Nogar and C. M. Kroninger, "Development of a Hybrid Micro Air Vehicle Capable of Controlled Transition," *IEEE Robot. Autom. Lett.*, vol. 3, no. 3, pp. 2269–2276, 2018, doi: 10.1109/LRA.2018.2800797.
- [51] Y. Lu, Z. Xue, G. S. Xia, and L. Zhang, "A survey on vision-based UAV navigation," *Geo-Spatial Inf. Sci.*, vol. 21, no. 1, pp. 21–32, 2018, doi: 10.1080/10095020.2017.1420509.
- [52] H. Ren, Y. Zhao, W. Xiao, and Z. Hu, "A review of UAV monitoring in mining areas: current status and future perspectives," *Int. J. Coal Sci. Technol.*, vol. 6, no. 3, pp. 320–333, 2019, doi: 10.1007/s40789-019-00264-5.
- [53] X. Yan, R. Chen, B. Lou, Y. Xie, A. Xie, and D. Zhang, "Study on Control Strategy for Tilt-rotor Aircraft Conversion Procedure," *J. Phys. Conf. Ser.*, vol. 1924, no. 1, 2021, doi: 10.1088/1742-6596/1924/1/012010.
- [54] G. S. Xia, M. Datcu, W. Yang, and X. Bai, "Information processing for unmanned aerial vehicles (UAVs) in surveying, mapping, and navigation," *Geo-Spatial Inf. Sci.*, vol. 21, no. 1, p. 1, 2018, doi: 10.1080/10095020.2017.1420510.
- [55] E. U. Rojo-Rodriguez, E. G. Rojo-Rodriguez, S. A. Araujo-Estrada, and O. Garcia-Salazar, "Design and Performance of a Novel Tapered Wing Tiltrotor UAV for Hover and Cruise Missions," *Machines*, vol. 12, no. 9, pp. 1–30, 2024, doi: 10.3390/machines12090653.
- [56] N. Mohammadi, M. Tayefi, and M. Zhu, "Vertical take-off and hover to cruise transition for a hybrid UAV using model predictive controller and MPC allocation," *Aircr. Eng. Aerosp. Technol.*, vol. 95, no. 10, pp. 1642–1650, 2023, doi: 10.1108/AEAT-04-2023-0090.
- [57] Z. Fang and A. V. Savkin, "Strategies for Optimized UAV Surveillance in Various Tasks and Scenarios: A Review," *Drones*, vol. 8, no. 5, 2024, doi: 10.3390/drones8050193.
- [58] A. Bin Junaid, A. D. D. C. Sanchez, J. B. Bosch, N. Vitzilaios, and Y. Zweiri, "Design and implementation of a dual-axis tilting quadcopter," *Robotics*, vol. 7, no. 4, pp. 1–20, 2018, doi: 10.3390/robotics7040065.
- [59] L. Zhong, H. Yuqing, Y. Liying, and H. Jianda, "Control techniques of tilt rotor unmanned aerial vehicle systems: A review," *Chinese J. Aeronaut.*, vol. 30, no. 1, pp. 135–148, 2017, doi: 10.1016/j.cja.2016.11.001.
- [60] Z. H. Cheng and H. L. Pei, "Transition Analysis and Practical Flight Control for Ducted Fan Fixed-Wing Aerial Robot: Level Path Flight Mode Transition," *IEEE Robot. Autom. Lett.*, vol. 7, no. 2, pp. 3106–3113, 2022, doi: 10.1109/LRA.2022.3145087.
- [61] A. C. Daud Filho and E. M. Belo, "A tilt-wing VTOL UAV configuration: Flight dynamics modelling and transition control simulation," *Aeronaut. J.*, vol. 128, no. 1319, pp. 152–177, 2024, doi: 10.1017/aer.2023.34.
- [62] X. ZHOU, X. ZHANG, B. WANG, and Q. ZHAO, "Aerodynamic and structural characteristics of helicopter rotor in circling flight," *Chinese J. Aeronaut.*, vol. 36, no. 12, pp. 282–296, 2023, doi: 10.1016/j.cja.2023.07.025.
- [63] C. Kang, S. Wang, W. Ren, Y. Lu, and B. Wang, "Optimization Design and Application of Active Disturbance Rejection Controller Based on Intelligent Algorithm," *IEEE Access*, vol. 7, pp. 59862–59870, 2019, doi: 10.1109/ACCESS.2019.2909087.
- [64] P. Casau, D. Cabecinhas, and C. Silvestre, "Hybrid control strategy for the autonomous transition flight of a fixed-wing aircraft," *IEEE Trans. Control Syst. Technol.*, vol. 21, no. 6, pp. 2194–2211, 2013, doi: 10.1109/TCST.2012.2221091.
- [65] I. Lopez-Sanchez and J. Moreno-Valenzuela, "PID control of quadrotor UAVs: A survey," *Annu. Rev. Control*, vol. 56, p. 100900, 2023, doi: 10.1016/j.arcontrol.2023.100900.
- [66] T. de J. Mateo Sanguino and J. M. Lozano Domínguez, "Design and stabilization of a Coandă effect-based UAV: Comparative study between fuzzy logic and PID control approaches," *Rob. Auton. Syst.*, vol. 175, pp. 1–14, 2024, doi: 10.1016/j.robot.2024.104662.
- [67] D. N. Cardoso, S. Esteban, and G. V. Raffo, "A new robust adaptive mixing control for trajectory tracking with improved forward flight of a tilt-rotor UAV," *ISA Trans.*, vol. 110, pp. 86–104, 2021, doi: 10.1016/j.isatra.2020.10.040.
- [68] M. Allenspach and G. J. J. Ducard, "Nonlinear model predictive control and guidance for a propeller-tilting hybrid unmanned air vehicle," *Automatica*, vol. 132, p. 109790, 2021, doi: 10.1016/j.automatica.2021.109790.
- [69] W. Tian, L. Liu, X. Zhang, and J. Shao, "Flight trajectory and energy management coupled optimization for hybrid electric UAVs with adaptive sequential convex programming method," *Appl. Energy*, vol. 364, p. 123166, 2024, doi: 10.1016/j.apenergy.2024.123166.
- [70] B. Wang, D. Zhu, L. Han, H. Gao, Z. Gao, and Y. Zhang, "Adaptive Fault-Tolerant Control of a Hybrid Canard Rotor/Wing UAV under Transition Flight Subject to Actuator Faults and Model Uncertainties," *IEEE Trans. Aerosp. Electron. Syst.*, vol. 59, no. 4, pp. 4559–4574, 2023, doi: 10.1109/TAES.2023.3243580.
- [71] Y. Zou, C. Liu, and K. Lu, "Robust smooth transfer for tilt-rotor aircraft under the asynchronous switching," *J. Franklin Inst.*, vol. 358, no. 18, pp. 9698–9720, 2021, doi: 10.1016/j.jfranklin.2021.10.016.
- [72] G. J. J. Ducard and M. Allenspach, "Review of designs and flight control techniques of hybrid and convertible VTOL UAVs," *Aerosp. Sci. Technol.*, vol. 118, p. 107035, 2021, doi: 10.1016/j.ast.2021.107035.
- [73] B. Sen Chen and T. W. Hung, "Integrating Local Motion Planning and Robust Decentralized Fault-Tolerant Tracking Control for Search and Rescue Task of Hybrid UAVs and Biped Robots Team System," *IEEE Access*, vol. 11, pp. 45888–45909, 2023, doi: 10.1109/ACCESS.2023.3273787.
- [74] J. Liao and H. Bang, "Transition Nonlinear Blended Aerodynamic Modeling and Anti-Harmonic Disturbance Robust Control of Fixed-Wing Tiltrotor UAV," *Drones*, vol. 7, no. 4, 2023, doi: 10.3390/drones7040255.
- [75] J. Wang, R. Chen, Z. Yu, and J. Lu, "Ground test and numerical investigation on aerodynamic performance of a quad tilt-rotor aircraft in ground and water effects," *Ocean Eng.*, vol. 289, no. P2, p. 116169, 2023, doi: 10.1016/j.oceaneng.2023.116169.
- [76] V. S. Chipade, Abhishek, M. Kothari, and R. R. Chaudhari, "Systematic design methodology for development and flight testing of a variable pitch quadrotor biplane VTOL UAV for payload delivery," *Mechatronics*, vol. 55, pp. 94–114, 2018, doi: 10.1016/j.mechatronics.2018.08.008.
- [77] H. Zhang, B. Song, F. Li, and J. Xuan, "Multidisciplinary design optimization of an electric propulsion system of a hybrid UAV considering wind disturbance rejection capability in the quadrotor mode," *Aerosp. Sci. Technol.*, vol. 110, p. 106372, 2021, doi: 10.1016/j.ast.2020.106372.
- [78] T. Patel, M. Kumar, and S. Abdallah, "Control of Hybrid Transitioning Morphing-wing VTOL UAV," *IFAC-PapersOnLine*, vol. 55, no. 37, pp. 554–559, 2022, doi: 10.1016/j.ifacol.2022.11.241.
- [79] N. T. Hegde, V. I. George, C. Gurudas Nayak, and K. Kumar, "Transition flight modeling and robust control of a VTOL unmanned quad tilt-rotor aerial vehicle," *Indones. J. Electr. Eng. Comput. Sci.*, vol. 18, no. 3, pp. 1252–1261, 2020, doi: 10.11591/ijeecs.v18.i3.pp1252b-cd.
- [80] N. Pavan, "Design of Tiltrotor VTOL and Development of Simulink Environment for Flight Simulations," *Indian Institute of Technology Madras*, 2020.